New Zealand Journal of Marine and Freshwater Research

ISSN: 0028-8330 (Print) 1175-8805 (Online) Journal homepage: http://www.tandfonline.com/loi/tnzm20

Currents off the west coast of Northland, New Zealand

PJH Sutton & MM Bowen

To cite this article: PJH Sutton & MM Bowen (2011) Currents off the west coast of Northland, New Zealand, New Zealand Journal of Marine and Freshwater Research, 45:4, 609-624, DOI: 10.1080/00288330.2011.569729

To link to this article: http://dx.doi.org/10.1080/00288330.2011.569729

New Zealand Journal of Marine and Freshwater Research
Vol. 45, No. 4, December 2011, 609–624

Taylor & Francis
Taylor & Francis Group

Currents off the west coast of Northland, New Zealand

PJH Sutton[a]* and MM Bowen[b]

[a]*National Institute of Water and Atmospheric Research Ltd, Kilbirnie, Wellington, New Zealand;* [b]*Victoria University of Wellington & GNS Science, Wellington, New Zealand*

(*Received 17 August 2010; final version received 4 December 2010*)

The concept of a southward-flowing West Auckland Current off the west coast of Northland has become an accepted feature of the ocean circulation around New Zealand. Knowledge of this flow is based on sparse data collected in the 1950s. Here we quantify the flows in the area for the first time using a current meter array deployed for a year (2003–2004) across the shelf and slope offshore of Hokianga Harbour and three hydrographic surveys along a transect coincident with the current meter array. Flows are found to be weak, and dominated by the variability. There is a southeastward drift in the mean flow offshore of the 1000-m isobath, with a northwestward mean found inshore of this. The offshore flows appear to result from large-scale sea surface height gradients, while the inshore flows respond to wind forcing in a complex manner.

Keywords: West Auckland Current; coastal currents; eastern boundary currents

Introduction

Currents along the northwest coast of New Zealand have previously been poorly measured. Despite the lack of study, this region is nationally significant. Ninety Mile Beach, at the northern end of the region, is critical for the green lip mussel aquaculture industry, with 80–90% of New Zealand's aquaculture mussels currently being grown from mussel spat harvested along this beach. Spat collection has been halted in the past because of harmful algal blooms in the area (Rhodes et al. 2001). Knowledge of the likely dispersal of such blooms is almost non-existent. There is also a significant inshore mixed trawl fishery for snapper, trevally, tarakihi and gurnard, along with a seasonal troll fishery for tuna. Finally, sand is extracted from the region, presently in Kaipara Harbour.

There are varied viewpoints in the historical literature of the flows off the west coast of northern New Zealand. From an analysis of some of 12,000 drift cards deployed in July 1953 to July 1954, Brodie (1960) shows that some cards released west of Cape Reinga in winter were recovered along the northwest coast of Northland, both north and south of Hokianga Harbour. For the other seasons, his figures show no evidence of a southward flow along the northwest coast. On the basis of this evidence (and earlier work by Garner, later described in Garner 1961), Brodie (1960) described the West Auckland Current (WAUC) as a flow from the north and west of Cape Reinga down the west coast towards the Kaipara Harbour. He did note, however, that southern drift cards deployed west of Cape Egmont and Farewell Spit showed northward trajectories, and pondered where and how the contrasting flows might meet.

From temperature and salinity distributions in a broad-scale hydrographic survey together with drift card releases, Garner (1961) concludes, 'a south-flowing tongue of subtropical

*Corresponding author. Email: p.sutton@niwa.co.nz

ISSN 0028-8330 print/ISSN 1175-8805 online

http://dx.doi.org/10.1080/00288330.2011.569729
http://www.tandfonline.com

water derived from the Trade Wind Drift, found off the west coast of North Island, is called the West Auckland Current'. Garner locates this southward flow *c.* 100 km offshore (although it is hard to know how literally his diagram should be interpreted).

Later work by Stanton (Stanton 1973a, 1973b) shows a change in thinking. His analysis was based on two hydrographic surveys and surface currents measured along a line running offshore from Reef Point using a Geomagnetic Electrokinetograph (GEK) towed behind a ship. Stanton (1973a) shows a southward WAUC, although in his figure it is placed closer to the coast (*c.* 40 km) than Garner had located it. Stanton (1973a) describes a predominantly northwestward coastal current, opposite in direction to the previously described WAUC and concludes: 'the present author is of the opinion that the predominant summer coastal current between Reef Point and Cape Reinga is northwestward.' (Reef Point is the small promontory southwest of Kaitaia; Fig. 1). Around the same time, Heath (1973) used the results of a nationwide broadscale hydrographic survey to interpret the flows along this coast as seasonally variable. He states that north of Cape Egmont flow is usually towards the north although a southwards flow may occur in winter (Heath 1973).

Later studies also emphasise a seasonal cycle in the currents. Ridgway (1980) concludes that the temperature and salinity properties as measured in grid surveys off the west coast of the North Island in August 1973 and February–March 1974 are consistent with a southward WAUC in winter but not in summer. Heath (1985) finds southward flows from current meter observations at 38°12′S 'under calm atmospheric conditions', but concludes that 'the direction of flow on the continental shelf north of Cape Egmont is not all clear.'

More recently, a southward-flowing WAUC, depicted as an inflow of subtropical water from the Tasman Front past Cape Reinga, was included on a chart representing mean surface flows around New Zealand (Carter et al. 1998) based on knowledge at that time. This chart represented the WAUC as being smaller and more variable than the East Auckland Current, which flows south eastward along the east coast of the North Island.

Placing the region in context, the northwest coast of New Zealand forms the eastern boundary of the Tasman Sea. The Tasman Front, a near zonal flow that connects the East Australian Current on the western side of the Tasman with the East Auckland Current, passes to the north of New Zealand and this study region. In the southern Tasman, the Subtropical Front approaches New Zealand at around 45°S before dipping south of New Zealand. Thus the study region is south of the main subtropical flow and north of the Subtropical Front.

In terms of possible important forcing mechanisms, eastern boundary currents often have a net poleward flow from rectification of poleward-travelling coastally trapped waves (CTWs), and in many cases the seasonal cycle of wind stress plays a leading role in the variability of the currents (Hill et al. 1998; Ridgway & Condie 2004). While CTWs have been observed further south along the west coast of the South Island (Cahill et al. 1991), propagation of wind energy around Cape Reinga is unlikely and local winds are generally weak.

Connection of the northwest coast to the deeper Tasman Sea is also limited by the shallow Challenger Plateau/Lord Howe Rise to the west. Energetic oscillations of the Tasman Front do occur at the northern end of the Caledonia Trough where the front approaches a gap in the Norfolk Ridge (*c.* 31°S, 168°E) (Stanton 1973a), but an examination of sea level anomalies (SLA) indicated little energy at the southern end of the trough where it meets the New Zealand coast.

In an attempt to clarify the confusion in the previous literature and elucidate the mechanisms that drive the currents along the northwest coast, an experiment was undertaken to study the flows with a long-term current meter deployment and shipboard transects. The data collected are discussed in the next section, along

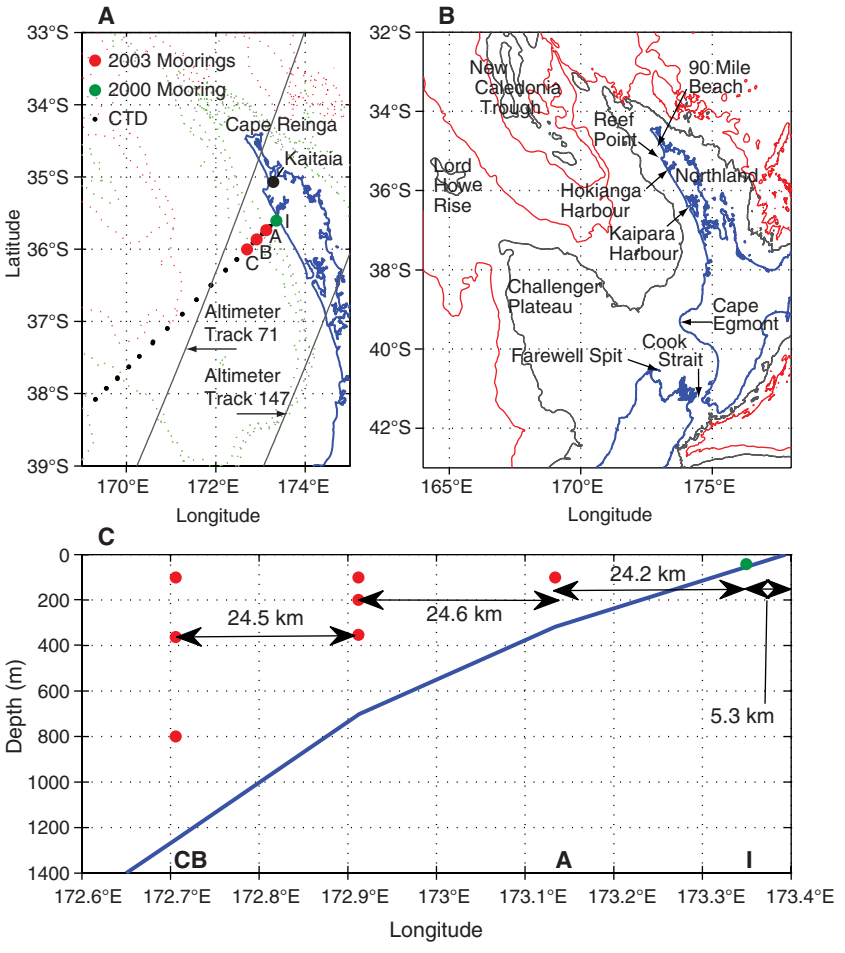

Figure 1 **A**, Locations of data. The 2003–2004 mooring locations are shown as the red dots, while the location of an earlier inshore mooring with 79 days of data from 2000 is shown as the green dot. Satellite altimeter tracks 71 and 147 are shown. The location of the Kaitaia EWS wind measurements is also shown. **B**, A larger scale map with locations mentioned in the text identified. The 1000-m and 2000-m isobaths are shown. **C**, The geometry of the mooring array, including the earlier inshore deployment.

with estimates of the current velocities and transports, then the mechanisms that could explain the measured flows are investigated. The observations and likely forcings are discussed in the conclusions.

Data

The focus of this study was a section offshore from Hokianga Harbour approximately perpendicular to the bathymetry and coastline (Fig. 1). This location was chosen to be along a relatively straight piece of coastline with relatively uniform bathymetry in order to ensure the local measurements were representative of the larger area. Also, the section aligned with an earlier inshore current meter deployment. There are no indications from any hydrographic or remotely sensed measurements of strong gradients or discontinuities along the northwest coast.

An array consisting of three moorings with a total of seven current meters was deployed offshore from Hokianga Harbour in July 2003 and recovered in August 2004 to measure the currents and their time variations. The mooring and current meter locations are shown in Fig. 1 and a summary of the data collected is given in Table 1. This current meter deployment is complemented by a previous inshore deployment along the same section (Fig. 1). Information about this shorter-duration inshore deployment is also included in Table 1. The offshore current meters were Aanderaa RCM-4 meters. Quoted accuracies for these meters are directional accuracies of $\pm 7.5^{\circ}$ for current speed between either 2.5 and 5 cm/s or 100 and 200 cm/s and $\pm 5^{\circ}$ for current speed between 5 and 100 cm/s, with speed accuracy of ± 1 cm/s or $\pm 2\%$ of the actual speed, whichever is greater. The Aanderaa RCM-4 current meters record an integrated speed throughout the sampling interval and an instantaneous direction. As such, they approximate a vector-averaging current meter. The inshore mooring had two InterOcean S4 current meters with stated directional accuracies of $\pm 2^{\circ}$ within tilt angles of 5° and speed accuracies of 2% of the reading or ± 1 cm/s.

The section along the line of the moorings was sampled three times: in September 2001, and during the current meter deployment and recovery voyages in July 2003 and August 2004. On each voyage, a CTD (Sea Bird Electronics SBE-19 plus) was used to measure profiles of salinity and temperature at the locations shown in Fig. 1. CTD processing is described in Walkington & Sutton (1997). Accuracies are $\pm 0.002^{\circ}$C and ± 0.005 for temperature and salinity, respectively.

In addition, a shipboard Acoustic Doppler Current Profiler (ADCP) (RDI Broadband 150 kHz) was used to measure the currents down to several hundred metres depth on each of the voyages. The measurement error in the ADCP velocity estimates is small, with the principal 'noise' in ADCP velocity estimates being variable flow such as wind-driven Ekman flow, near inertial currents and tides. A detailed description of the ADCP processing and error analysis can be found in Sutton & Chereskin (2002). Tidal currents were removed from the ADCP measurements by calculating the tide at each position and time using a tide model, and then subtracting the result from the data. The tide model used is a high-resolution barotropic tidal model of the New Zealand region as described in Walters et al. (2001). The model has been shown to reproduce velocities accurately (Stanton et al. 2001) and qualitative comparisons with high-pass filtered currents from this data set are favourable. Note that there is no means to filter out other high-frequency variability such as inertial motion from the ADCP measurements, and this must be taken into account when comparing the

Table 1 Current meter locations and data records.

Meter name	Latitude	Longitude	Water depth (m)	Meter depth (m)	Date of first good data	Date of last good data	Data record length (days)
I1	35°36.34′S	173°20.95′E	56	33	5-Apr-2000	23-Jun-2000	79.0
I2	35°36.34′S	173°20.95′E	56	52	5-Apr-2000	23-Jun-2000	79.0
A1	35°44.12′S	173°08.05′E	317	97	16-Jun-2003	17-Aug-2004	335.0
B1	35°51.90′S	172°54.77′E	701	101	17-Jul-2003	2-Aug-2004	382.0
B2	35°51.90′S	172°54.77′E	701	201	17-Jul-2003	2-Aug-2004	381.5
B3	35°51.90′S	172°54.77′E	701	351	17-Jul-2003	2-Aug-2004	382.0
C1	36°00.55′S	172°42.37′E	1253	103	17-Jul-2003	16-Nov-2003	122.5
C2	36°00.55′S	172°42.37′E	1253	353	17-Jul-2003	31-Jan-2004	198.5
C3	36°00.55′S	172°42.37′E	1253	803	17-Jul-2003	25-Jan-2004	192.0

ADCP results with filtered current meter results and geostrophic calculations.

Wind data were extracted from the NIWA Climate Data Base (http://cliflo.niwa.co.nz/). Several sites were examined to determine how representative they were of larger-scale conditions. The data presented here are from the Kaitaia Aero EWS station (agent number 18183, network number A53026, −35.067°S, 173.287°E). Hourly wind speed and direction are collected at the location shown on Fig. 1, at an altitude of 80 m above sea level. Data from this site span the early inshore mooring deployment as well as the later offshore deployments.

The analyses in this paper will be discussed in terms of parallel to (alongshore) and perpendicular to (cross-shore) the coastline/bathymetry, i.e. in a rotated coordinate system with positive signs corresponding to towards shore and 'northward' alongshore flows. The wind data are similarly rotated, and a sign change is included to make the winds follow the standard oceanographic convention of 'direction to' rather than 'direction from' (i.e. a southerly wind becomes a northward flow).

Along-track satellite sea surface height data were used to investigate larger-scale oceanic forcings. The Jason-1 satellite altimeter tracks cross north (track 71) and south (track 147) of the current meter array (Fig. 1), and provide estimates of SLA every 10 days. The SLA along these tracks were obtained from the JPL Physical Oceanography Distributed Active Archive Center (http://podaac.jpl.nasa.gov) and have the standard corrections applied (AVISO 1998).

The SLA data cannot provide estimates of mean pressure gradients but they can be used to estimate the variability of the cross-shore and alongshore pressure gradients. Variability of the cross-shore pressure gradient was derived by smoothing and differencing the SLA along track 71 over five points (30 km) and averaging the resulting slope between the 1700-m and 1000-m isobaths (11 points). Variability in the alongshore pressure gradient was estimated by averaging the SLA between the 200 m and 1500 m along each track and differencing the averages between the tracks. In both cases, the SLA differences were smoothed over three points in time (30 days). Individual SLA measurements are accurate to ±4 cm. Using standard error propagation, the SLA differences are accurate to less than ±1 cm. The SLA tracks are not sampled simultaneously. However, the 30-day running mean smoothing means that the time difference between the samplings does not affect the analysis.

Results

Currents from shipboard transects

The flows measured were variable and showed significant structure. The three ADCP surveys (Fig. 2) and the geostrophic velocities calculated from the three CTD surveys (Fig. 3) provide spatial context and give an insight into the current meter measurements. The geostrophic calculations were referenced to a level of no motion at the bottom. This is undoubtedly only an approximation, but the CTD, ADCP and current meter data indicate that the flows in the region are weak, variable and surface-intensified. Thus the geostrophic flows referenced to the bottom should be a useful estimate of the alongshore geostrophic currents through the water column. The ADCP measurements show changes in the flow structure along the section, with banding in the velocity structure. In particular, the inshore part of the section tends to have reversed flow compared with the offshore. Flows measured were typically 30 cm/s or less. The geostrophic calculations also show changes in the flow structure along the section, with a tendency for southward flow offshore (west of 172.6°E) and northward flow inshore with some 'banding'. The CTD station spacing (Fig. 3) barely resolves the finer-scale flow field, but does resolve the broader scales, e.g. the southward offshore and northward inshore flow patterns in 2001 and 2004.

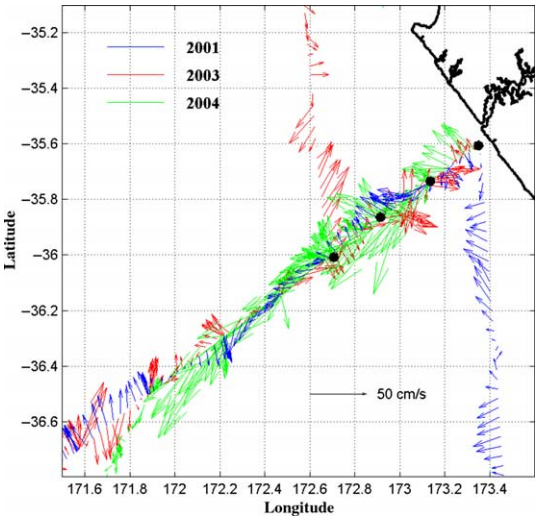

Figure 2 Velocities at 40-m depth as measured by the vessel mounted Acoustic Doppler Current Profiler (ADCP) during the three voyages in September 2001, July 2003 and August 2004 with tides removed (see data section for details).

Currents from moored measurements

The moored current meters give information about temporal variability. There is a strong tide along this coast, particularly the M2 component, and mean tidal velocities measured by the current meters are *c.* 7 cm/s, consistent with predictions from the tidal model (Walters et al. 2001). For the offshore three moorings, high-frequency flows (tides and inertial motion) are responsible for an average of around 60% of the variance in the cross-shore flows and 55% of the alongshore variance. In contrast, the high-frequency flows only account for about 20% of the variance in both directions at the earlier inshore mooring. To study the low-frequency flows, the tidal and inertial flow contributions were removed by low-pass filtering with a 24-h filter (24m214 from Thompson 1983).

The alongshore and cross-shore components of the detided currents are shown in Fig. 4 and the basic statistics are given in Table 2. Note that the two earlier inshore meters (I1 and I2) had a faster sampling rate than the later offshore deployment. To obtain standard deviations comparable with the quasi vector-averaged results from the offshore RCM-4 current meters, the inshore data were smoothed with a running mean and then subsampled to match the time resolution of the offshore meters before the standard deviations were calculated. The mean current directions for each meter along with an ellipse showing one standard deviation for the detided time series are shown in Fig. 5. The different depths of the meters are indicated by the colours, with red being the shallowest meters, green the intermediate meters and black the deepest meters. Note that these results are based on all of the data collected at each meter and therefore are not for the same data periods (see Table 1 for the length of the respective time series).

Almost without exception, the standard deviations are larger than the mean (the exceptions being the cross-shore flow at the bottom current meter on mooring B (B3) and the alongshore flows at the top two meters on mooring C (C1 and C2). There is shoreward mean flow at all meters except the near-bottom inshore meter (I2). The inshore moorings (I and

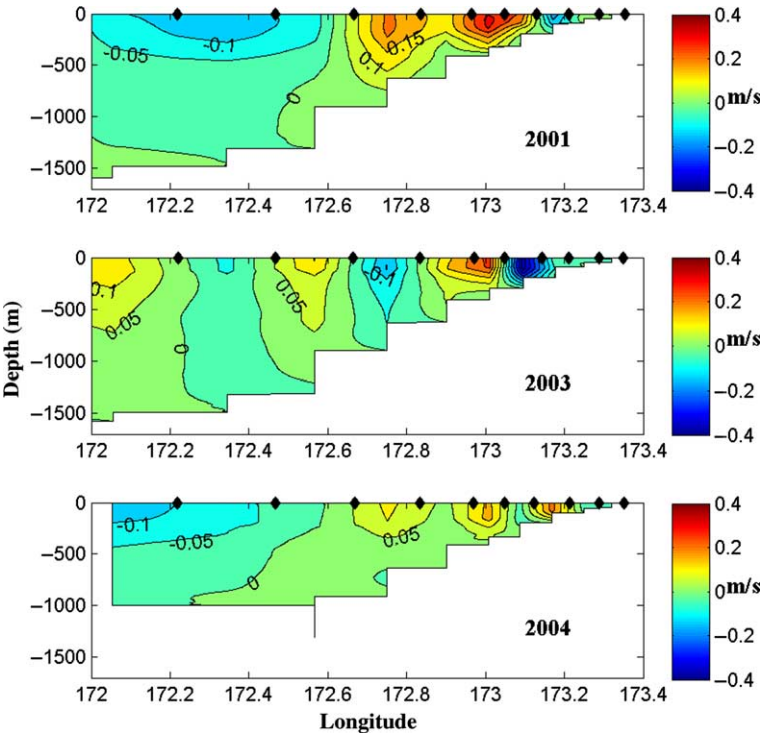

Figure 3 Geostrophic velocities referenced to the bottom from the three CTD transects: September 2001, July 2003 and August 2004. Positive is northwards flow, i.e. into the page. The locations of the CTD stations are shown by the diamonds along the top axes.

A) shows northward alongshore mean flow, while the meters on the offshore two moorings (B and C) all have southward means.

The detided flows at the various moorings show varying correlations (Table 3). Note that because the time series have differing lengths, these statistics are not directly inter-comparable, but are an indication as to the across-shelf length scales of the flows.

These correlations indicate that both the cross-shore and alongshore currents are correlated vertically on each mooring. There are higher correlations between moorings for the cross-shore flow than for the alongshore, but there is some correlation between the B and C moorings for the alongshore flow as well. The data from mooring A are not well correlated with any of the other measurements. The earlier inshore mooring could not be included in this analysis, as the data are not contemporaneous.

The correlations between the C1 record and the other measurements give the ability to extend the short C1 record synthetically, which greatly improves later analyses of currents and transport variability. Analysing the variability in the C1 record indicates that 84% of the cross-shore variance and 69% of the alongshore variance in the C1 record can be explained through a linear combination of the other six simultaneous current meter measurements. This variance accounted for increases to 91% cross-shore/81% alongshore for a 3-day smoothed product, and 96% cross-shore/92% alongshore for a 10-day smoothed product. The 12-hourly and 10-day smoothed currents along with the fits are shown in Fig. 6. The proportion of variance fitted justifies extending the short C1 record through to 25 January 2004, when C3 fails, particularly to study lower frequency

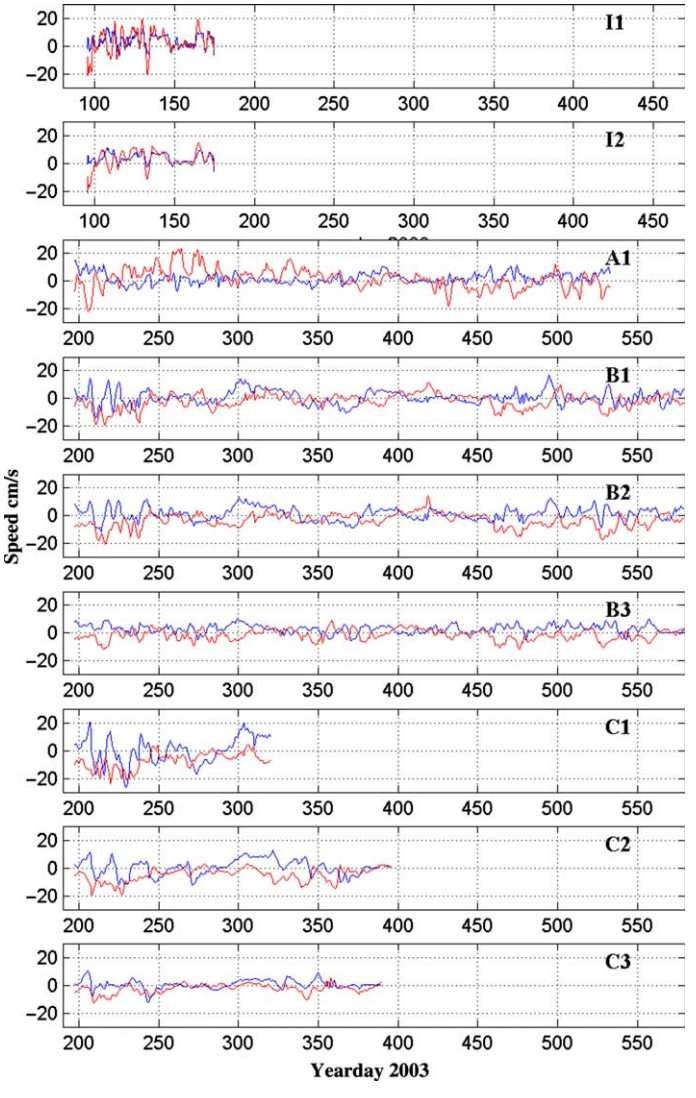

Figure 4 The cross-shore (blue) and alongshore (red) components of the detided currents measured by the meters. The sign convention is positive eastward for the cross-shore, and positive northward for the alongshore. Note that the two upper panels for the inshore mooring are for year 2000. The time scale divisions are the same.

processes. This extension is done by fitting the measured data up until 16 November 2003 with a least-squares fit from the remaining data. The coefficients from this fit are used to reconstruct the C1 record between 16 November 2003 and 25 January 2004.

Along-shore transport from moored measurements

A simple estimate of the alongshore transport during the 2003 moorings deployment was calculated by dividing the coastal wedge into areas, with the divisions being halfway between

Table 2 Means and standard deviations of the cross-shore and alongshore components of the detided flows.

	Cross-shore		Alongshore	
	(u') (cm/s)	$\sigma(u')$ (cm/s)	(v') (cm/s)	$\sigma(v')$ (cm/s)
I1	3.84	4.78	2.85	8.18
I2	−0.72	2.58	3.98	7.52
A1	1.91	3.72	1.59	7.27
B1	0.62	4.93	−2.02	5.18
B2	1.14	4.68	−3.74	5.09
B3	2.97	2.93	−1.49	3.80
C1	0.25	9.45	−7.18	6.02
C2	0.26	5.68	−5.04	4.80
C3	0.54	3.25	−2.45	3.19

each current meter. This is equivalent to linear interpolation between the current meters and persistence beyond the meters. The transport calculations are broken into two regions, with the inshore mooring (A) being treated in isolation, and the offshore moorings (B and C) being combined, reflecting the correlations described above. The resulting transports are shown in Fig. 7 for the detided data both with and without a 10-day running mean filter. The inshore transport is northward for the first half of the record and then southward for the second, with a mean inshore transport of 0.5 Sv (northward) and a standard deviation of 0.7 Sv. The offshore transport is almost entirely southward with a mean transport of −1.6 Sv (southward) and a standard deviation of 1.2 Sv.

The previous studies of the WAUC postulate southward flows in winter (Brodie 1960; Heath 1973; Ridgway 1980). The offshore flows in this record are indeed southward in winter (taken to be June, July, August or year days 151–241), but the inshore flow is weak and changes sign through this period. However, the offshore flow continues to be southward through to summer (taken to be December, January, February or year days 334–423): counter to the northward flows stated by Heath (1973) and Ridgway (1980). Also, the north-westward summer coastal current described by Stanton (1973a, 1973b) is not evident in this

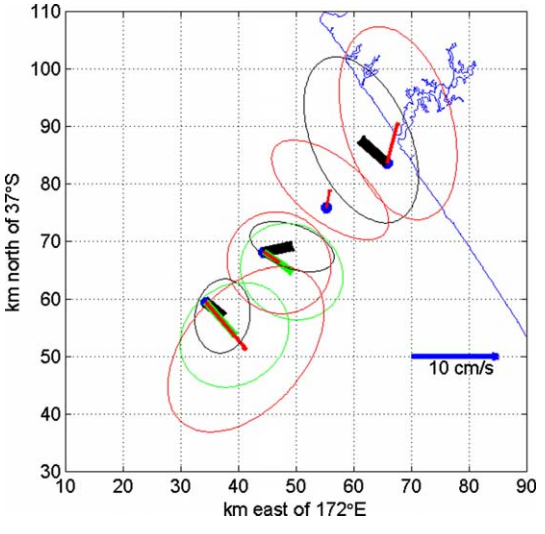

Figure 5 The mean currents from each current meter record are shown as the quivers. The ellipses denote one standard deviation once the data have been detided. The different levels are shown by the colours, with red being the shallowest meters, green the intermediate meters and black the deepest meters. Note that these results are based on all of the data collected at each meter and therefore are not for the same data periods (see Table 1 for the length of the respective time series).

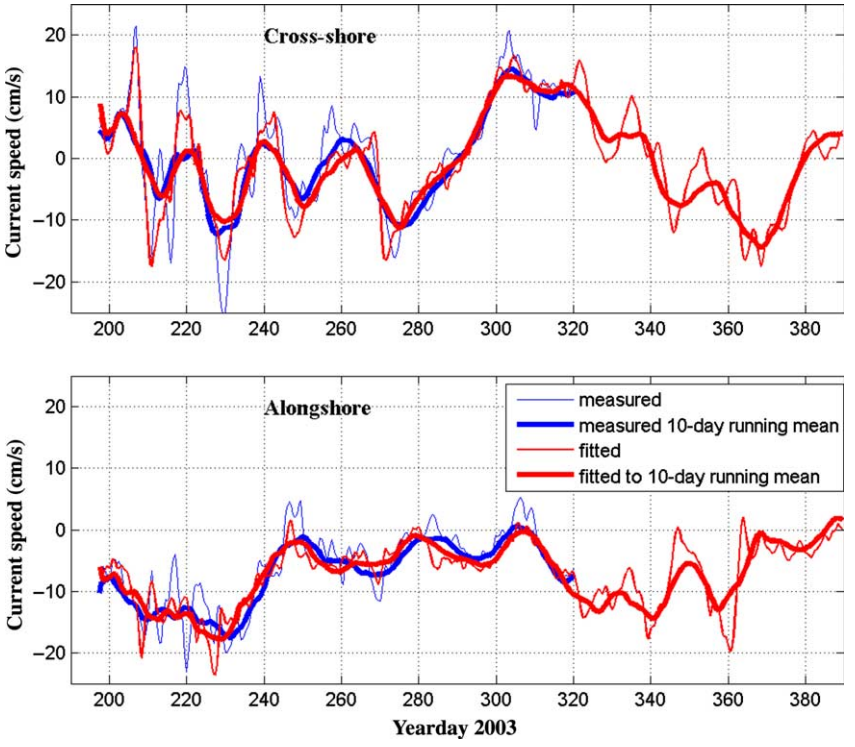

Figure 6 Reconstructing and extrapolating C1 from the other current meters. The thin blue lines show the detided cross-shore and alongshore components as measured by C1. The thick blue line shows the 10-day running means. The fits to the detided data and 10-day smoothed data are shown by the thin and thick red lines respectively.

dataset. Thus, while this dataset is clearly too short to resolve any annual cycle, these measurements do bring into question the seasonality suggested in previous descriptions of the currents in this region.

Forcing mechanisms

The currents and transports are obviously highly variable, with the variance being of the order of the mean even for detided and 10-day smoothed data. Local wind stress and deep ocean flows are likely candidates for driving the flows along the slope and shelf. Effects of local wind stress are examined by comparison with the cross-shore and alongshore winds measured at Kaitaia, converted to wind stress (Gill 1982). Interestingly, the mean wind stress along this coast is almost exactly cross-shore, i.e. there is minimal mean alongshore wind stress. Deep ocean forcings are addressed by comparison with the cross-shore and alongshore gradients in SLA. High-resolution along-track data from track 71 and 147 were used as explained previously to estimate the along-shore gradient (the 'head') and the cross-shore gradient (the 'slope'). The forcing time series used in the analyses are shown in Fig. 8.

A local alongshore wind stress is expected to create an alongshore geostrophic flow (Gill 1982), although differences in stratification and bathymetry can create markedly different types of density and current structures (Hill et al. 1998). Persistent slopes in sea level would be expected to correspond to geostrophic flows. Note that alongshore slopes can induce

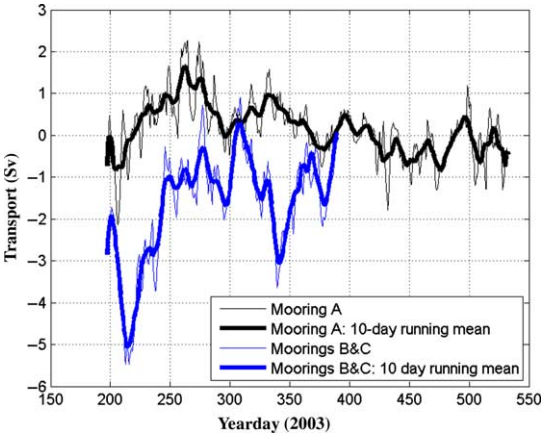

Figure 7 Alongshore transports from 2003 mooring deployments. Black line = inshore mooring (A), blue = offshore two moorings (B and C). Heavier lines are smoothed with a 10-day running mean. Positive is northwestward, negative southeastward. Note that the offshore transport is calculated using the 'extended' C1 record.

cross-shelf slopes, so the two components of pressure gradient are not independent (Hill et al. 1998). Indeed, wind stress also generates sea level gradients, so the four forcing parameters are neither independent nor orthogonal. While the forcing time series are correlated to some degree, they are not so correlated as to be redundant. The highest correlation is between the alongshore wind stress and the alongshore SLA gradient which has a negative correlation coefficient of −0.59.

Table 3 Correlations between detided time series.

	A1	B1	B2	B3	C1	C2	C3
A1	1	0.19	0.18	0.35	0.19	0.16	−0.02
B1	0.24	1	**0.82**	*0.41*	**0.70**	**0.55**	0.16
B2	0.33	**0.86**	1	**0.54**	**0.74**	**0.59**	0.14
B3	0.30	**0.63**	**0.75**	1	**0.53**	0.40	0.12
C1	0.28	*0.48*	*0.43*	0.18	1	**0.87**	*0.47*
C2	0.21	0.39	0.29	0.01	**0.80**	1	*0.48*
C3	0.20	0.38	0.33	0.23	0.37	*0.47*	1

The upper half of the table (i.e. above the diagonal) is for the cross-shore component of the flow (u), while the lower half is for the alongshore (v). As a visual guide, correlations between 0.4 and 0.5 are in italics, while those above 0.5 are in bold.

The approach taken for the offshore moorings (A, B and C) was to investigate the relationships between the data and the four forcing candidates, i.e. the alongshore and cross-shore wind stresses and the alongshore and cross-shore SLA gradients. A variety of temporal smoothings was experimented with, with the results being consistent for smoothing longer than the 10-day SLA sampling rate. To be consistent with this 10-day resolution in the SLA and three-point smoothing used in defining the slopes, all of the time series (data and forcing) were smoothed with a 30-day running mean.

Figure 9 shows how much of the alongshore and cross-shore variance from current meter records can be accounted for by the four parameters. As the parameters are not orthogonal, the technique used was stepwise multiple linear regression. The data time series was regressed onto each of the forcing parameters in turn. Once the parameter that could account for the highest variance was identified, the time series was then regressed onto a pairing of this first parameter and each of the other parameters, to identify the second parameter that when included with the first could account for

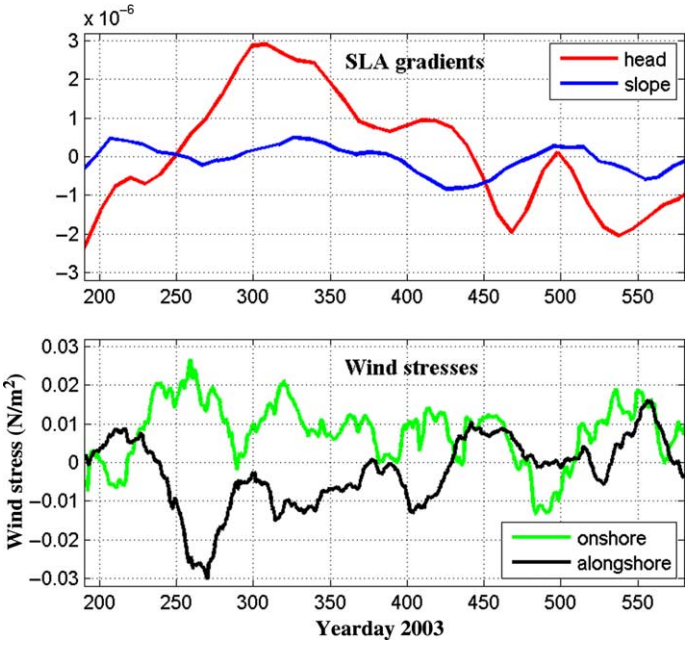

Figure 8 The time series used to investigate likely forcing mechanisms: the cross-shore (slope) and alongshore (head) gradients in sea level anomalies (SLA), and the cross-shore and alongshore components of the wind stress smoothed with a 30-day running mean.

the most variance. Once this was done, the first two parameters were used together with each of the remaining two to find which of the remaining parameters accounted for the most variance. The results of the stepwise linear regression should be taken as indicative and suggestive. The limitations of the dataset and low signal to noise made this simple and somewhat crude analysis appropriate; more sophisticated approaches could not be supported by the data.

Looking first at the alongshore current components, the variance in the offshore meters (C1 to C3) is well captured, with 78–85% of the variance being able to be explained by the four parameters. The SLA slope and head dominate, accounting for 70–83% of the variance. The SLA slope could be expected to define the alongshore currents in a geostrophic sense, and indeed the SLA slope accounts for most of the alongshore variance on the C1 and C2 records. Similarly, any geostrophic component in the cross-shore flows would be defined by the alongshore SLA gradient (the SLA head). The SLA head does dominate for the cross-shore flows at C1, C2 and C3, and also accounts for the most variance for the alongshore flow at the bottom C3 meter. The changes in the relative importance of the SLA head and SLA slope for the alongshore flow at the bottom meter (C3) could perhaps be a result of topographic effects. The alongshore and cross-shore wind stresses do not contribute significantly or consistently to these C1, C2 and C3 records.

Moving inshore to the middle meters (B1 to B3), there is a vastly different ability to account for the alongshore and cross-shore current variabilities. For the alongshore flow, while the SLA head and slope are the best of the options in explaining the variance, the amount of variance they can explain has fallen: to around 54% for B1, back up at 71% for B2 and then only 38% for B3. For this alongshore flow at these B meters, the SLA slope and SLA

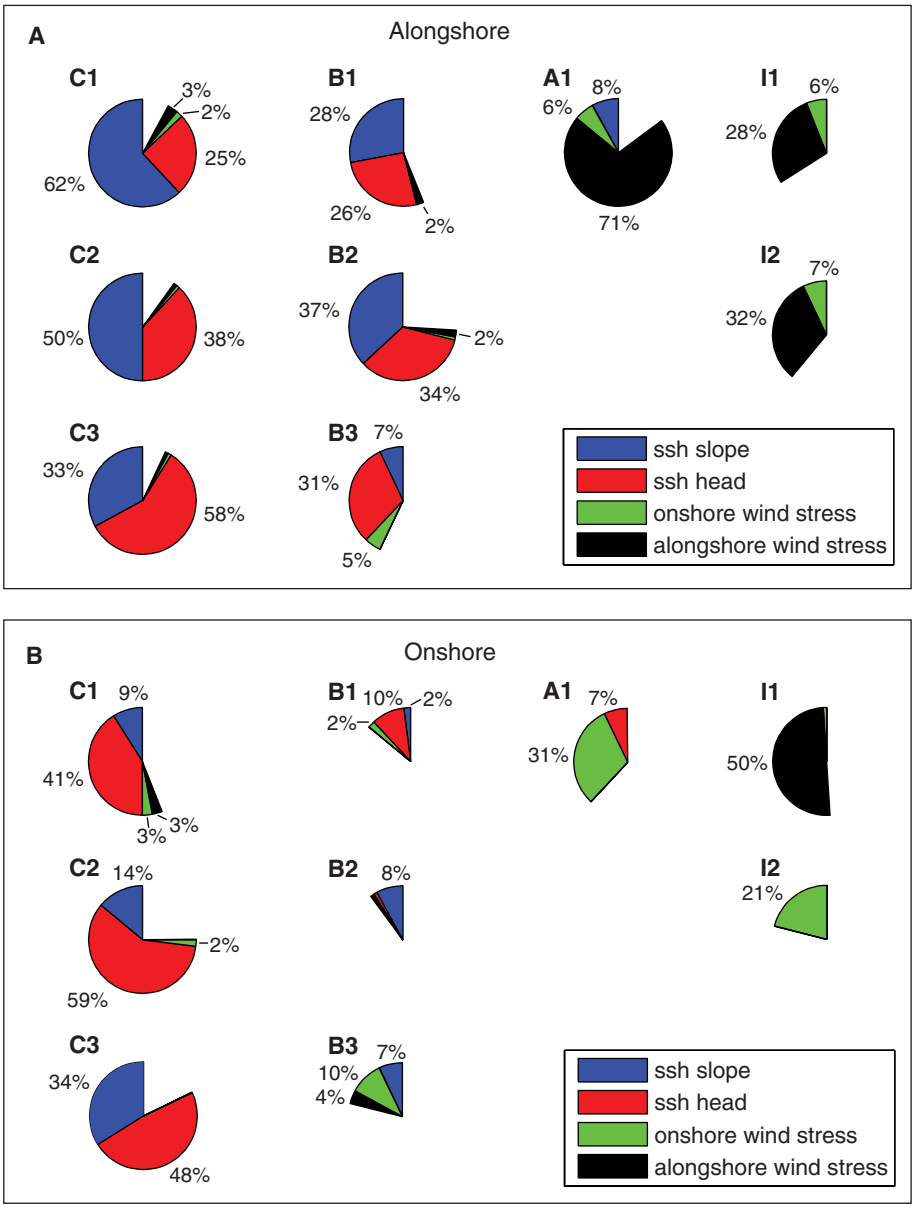

Figure 9 The variance accounted for by the cross-shore and alongshore winds and cross-shore (slope) and alongshore (head) sea level anomaly (SLA) gradients is investigated by serially regressing the time series against the parameters to find the combination that accounted for the most variance (see text for details).

head contribute roughly equally, while the wind stresses again explain little of the variance. The cross-shore flow variability at the B meters is very poorly accounted for by the four parameters.

Moving to the alongshore flows at the inshore meter A, we see a large change in behaviour. Here the alongshore current variability can be well explained by the alongshore wind stress. Intriguingly, the currents

are anticorrelated with the alongshore wind stress, i.e. the positive (northward) signal in the currents seen in Fig. 4 around year day 260–270 corresponds to a period of southward wind stress, and conversely a later period of negative current flow (around year day 475) corresponds to a period of positive winds. The cross-shore flows at mooring A are somewhat correlated with the cross-shore winds, although only 31% of the variance can be accounted for. The SLA parameters explain little of the variance at mooring A.

The inshore mooring was treated individually. Satellite SLA could not give accurate estimates of the SLA in water this shallow, and winds could be expected to dominate. Given the shorter time scales associated with winds and the short (79-day) deployment, a 10-day running mean was used. Wind forcing can account for a significant amount of the variability in the alongshore (34–39%) and cross-shore (21–50%) flows, with the alongshore wind stress being dominant, except for the cross-shore flow at the bottom meter. Unlike mooring A, the alongshore current variability is positively correlated with the alongshore wind stress variability. Comparing the alongshore flow with the alongshore wind stress indicates that some wind events are clearly reflected in the current field, while others are not. The fields are related, but not simply or linearly.

Other forcing mechanisms were considered and investigated. CTWs can also create a rectified flow in the direction of propagation (poleward); however, with this region being at the northern limit of the west coast of New Zealand, it could be a formation region for CTWs but is unlikely to be remotely forced. CTWs have been studied off the west coast of South Island, but these waves were found to be forced from the Cook Strait/Taranaki Bight area—well south of this region (Cahill et al. 1991). In addition, non-linear relationships were investigated, including separating the northward along coast and southward along coast forcing mechanisms and responses and analysing each direction separately. No significant relationships were found. This may be related to the relatively limited temporal extent of the dataset, or perhaps more to low signal to noise in this relatively quiescent region.

Discussion

Previous papers have described a southeastward current off the west coast of Northland, New Zealand called the WAUC (Brodie 1960; Garner 1961). Other authors have stated that this flow is seasonal (Stanton 1973a, 1973b; Heath 1973; Ridgway 1980). A later paper (Heath 1985) states that the direction of flow in this region is 'not at all clear'. The most recent mention of the current indicates a southeastward WAUC (Carter et al. 1998).

The data presented here represent the first measurement campaign in the region since the 1950s. These modern data indicate that the region is one of weak flows, where the variability at tidal and intra-annual time scales dominates. Typical offshore mean flows are indeed southeastward, consistent with a WAUC, and are of the order of 3–8 cm/s. This should be interpreted in the context of variability at time scales greater than a day of the same order, and typical tidal and inertial motion variability (i.e. time scales less than a day) of the order of 6 cm/s.

Inshore flows, in water less than 1000 m deep are more complicated. In fact one of the most consistent signals in this dataset is 'banding' in the flow structure, with bands of weakened, intensified and even alternating flows inshore of the 1000-m isobath. These bands are clear in the ADCP sections (Fig. 2) and CTD-calculated geostrophic flow sections (Fig. 3). Impacts of the banding in the flow field are apparent in the current meter data. The offshore mooring (C) is in the predominantly southeastward offshore regime, while the middle mooring (B) is correlated with the offshore mooring, but appears to be near a transition between the offshore flow and a more complicated inshore field. Thus the current meters on B have lower mean flows than

those on C (Table 2), and the variability at these meters is not as well accounted for by the forcing mechanisms investigated. The very inshore current meters (on mooring A and the earlier coastal deployment I) show northwestward mean flow of *c.* 2–4 cm/s, but again, this should be interpreted in light of variability at time scales greater than a day of 7–9 cm/s and tidal and inertial variability of 7–10 cm/s.

Corresponding to the changing structure between the offshore and inshore flows is an apparent change in the likely forcing (Fig. 8). The offshore current variability appears to be forced in a largely geostrophic manner by larger-scale changes in sea surface height. Moving inshore, changes in wind stress account for the most variance. There are some non-trivial aspects to the wind forcing, however, with the alongshore currents at mooring A being strongly anticorrelated with the alongshore winds, but those at the very shallow mooring I being positively correlated with the alongshore winds.

In an effort to gain a larger-scale view of the area, surface trajectories from surface drifters from The Global Drifter Program (http://www.aoml.noaa.gov/phod/dac/index.php) and *c.* 1000-m trajectories from Argo floats (http://www.argo.ucsd.edu/) were examined. In fact, no Argo floats to date have traversed the area west of Northland, and the few surface drifters that have sampled the region have shown slow eastward drifts before beaching along the coast. Thus, this region appears to be a bit of a cul-de-sac in the regional ocean, consistent with the weak and variable flows found in this study.

In summary, the West Auckland area is a region of weak flows dominated by variability at time scales both less than 1 day (tidal and inertial) and greater than 1 day (Fig. 5). There was a weak southeastward flow offshore of the 1000-m isobath through the study period (Fig. 7). Inshore flows were spatially highly structured (Fig. 2 and 3) and are even more dominated by variability (Fig. 5), with a northward mean flow near the coast. There was no sign of seasonal variability, although the dataset was too short to adequately resolve this.

So is there a WAUC? Perhaps in water deeper than 1000 m, although the weakness of the flows and degree of variability mean that this current has probably been overstated in previous literature. A better interpretation would be that the area has typically weak flows that are dominated by the variability with a southeastward tendency offshore of the 1000-m isobath and an even weaker and more variable northward tendency inshore.

Acknowledgements

We thank the captain and crew of RV *Tangaroa* for their work on the oceanographic surveys. Special thanks to the NIWA mooring group (M. Greig and W. Main) the CTD technician (M. Walkington) and ADCP technician (A. Falconer). Rob Bell and Rick Liefting provided the inshore mooring data. This research was funded by Foundation for Research, Science and Technology contract C01X0202 and C01X0701.

References

AVISO 1998. AVISO User handbook: sea level anomaly files, CNES project document, AVI-NT-011-312-CN, Edition 3.1.

Brodie JW 1960. Coastal surface currents around New Zealand. New Zealand Journal of Geology and Geophysics 3: 235–252.

Cahill ML, Middleton JH, Stanton BR 1991. Coastal-trapped waves on the west coast of South Island, New Zealand. Journal of Physical Oceanography 21: 541–557.

Carter L, Garlick RD, Sutton P, Chiswell S, Oien NA, Stanton BR 1998. Ocean Circulation New Zealand. NIWA Chart Miscellaneous Series No. 76.

Garner DM 1961. Hydrology of New Zealand coastal waters, 1955. New Zealand Department of Scientific and Industrial Research Bulletin 138. New Zealand Oceanographic Institute Memoir No. 8.

Gill AE 1982. Atmosphere-ocean dynamics. International Geophysics Series 30. London, Academic Press.

Heath RA 1973. Present knowledge of the oceanic circulation and hydrology around New Zealand—1971. Tuatara 20: 125–140.

Heath RA 1985. A review of the physical oceanography of the seas around New Zealand—1982. New Zealand Journal of Marine and Freshwater Research 19: 79–124.

Hill AE, Hickey BM, Shillington FA, Strub PT, Brink KH, Barton ED, Thomas AC 1998. Eastern ocean boundaries, coastal segment (E). In: Robinson AR, Brink KH, ed The sea, Vol. 11, The global coastal ocean: regional studies and syntheses, Chap. 2. New York, John Wiley & Sons. Pp. 29–67.

Rhodes LL, MacKenzie AL, Kaspar HF, Todd KE 2001. Harmful algae and mariculture in New Zealand. Short communication. ICES Journal of Marine Science 58: 398–403.

Ridgway NM 1980. Hydrological conditions and circulation off the west coast of the North Island, New Zealand. New Zealand Journal of Marine and Freshwater Research 14: 155–167.

Ridgway KR, Condie SA 2004. The 5500-km-long boundary flow off western and southern Australia. Journal of Geophysical Research 109: C04017, doi:10.1029/2003JC001921.

Stanton BR 1973a. Circulation along the eastern boundary of the Tasman Sea. Oceanography of the South Pacific 1972, comp. R Fraser. New Zealand National Commission for UNESCO, Wellington.

Stanton BR 1973b. Hydrological investigations around northern New Zealand. New Zealand Journal of Marine and Freshwater Research 7: 85–110.

Stanton BR, Goring DG, Bell RG 2001. Observed and modelled tidal currents in the New Zealand region. New Zealand Journal of Marine and Freshwater Research 35: 397–415.

Sutton PJH, Chereskin TK 2002. Absolute geostrophic currents in the East Auckland Current region. New Zealand Journal of Marine and Freshwater Research 36: 751–762.

Thompson R 1983. Low-pass filters to suppress inertial and tidal frequencies. Journal of Physical Oceanography 13: 1077–1083.

Walkington CM, Sutton PJH 1997. CTD data report from East Auckland Current Cruise IV. NIWA Physics Section Report 97–3. Wellington.

Walters RA, Goring DG, Bell RG 2001. Ocean tides around New Zealand. New Zealand Journal of Marine and Freshwater Research 35: 567–579.